Phonon density of states of silicon clathrates: Characteristic width narrowing effect with respect to the diamond phase

P. Mélinon, P. Kéghélian, and A. Perez
Département de Physique des Matériaux, Université Claude Bernard-Lyon 1, 69622 Villeurbanne, France

B. Champagnon, Y. Guyot, and L. Saviot
Laboratoire de Physico Chimie des Matériaux Luminescents, Université Claude Bernard-Lyon 1, 69622 Villeurbanne, France

E. Reny, C. Cros, and M. Pouchard
Institut de Chimie de la Matière Condensée de Bordeaux, Université Bordeaux I, 33608 Pessac, France

A. J. Dianoux
Institut Laue Langevin, Boîte Postale 156, Grenoble Cédex 9, France
(Received 21 October 1998)

The phonon density of states of different silicon clathrate phases is measured by inelastic neutron scattering. M_x@Si-34 and M_x@Si-46 clathrates with different alkaline (M=Na, K) and composition x are investigated. A width-narrowing effect is observed on the phonon spectra with respect to the diamond silicon structure. The effect of the alkali atom-silicon atom coupling is seen demonstrating the strong interaction between the alkali-atom and the host silicon cage. Such specific properties of clathrate lattices are interpreted in term of local icosahedral symmetry. [S0163-1829(99)02415-7]

I. INTRODUCTION

Fullerene-assembled solids have been extensively studied over the past decade.[1] For example, in C_{60} solids,[2] the polyhedra are held together by weak van der Waals interactions leading to a strong molecular signature of such polyhedra into the solid. Other cagelike assembled materials so called ''clathrates'' were synthesized thirty years ago.[3] They are the subject of growing interest at the present time mainly related to the observation of superconducting behavior in Na_xBa_y@Si-46 clathrate phase.[4] Clathrates labeled Si-46 ($Pm\bar{3}n$ symmetry) and Si-34 ($Fd\bar{3}m$ symmetry) are built from the regular arrangement of a combination of Si_{20} (I_h) and Si_{24} (D_{6d}) or Si_{28} (T_d) cages, respectively. Additional atoms such as alkaline or barium are included in the cages, leading to a doped semiconductor behavior. Furthermore, it has been pointed out that the electronic structure of pure Si clathrate seems promising for optoelectronic applications.[5] Contrary to fullerene-assembled solids, in the clathrate phases the silicon cages are linked together by strongly covalent bonding since the polyhedra share pentagonal and hexagonal faces. Such lattices, which present a nearly perfect sp^3-hybridized tetrahedral symmetry are *true covalent* crystals with expected ''broad'' bands while fullerene solids present the molecular signature of the individual cages. Moreover, recent calculations have shown a wide band-gap opening in the electronic density of states (e-DOS) of clathrates, which is partially attributed to the parity of the member rings.[5–7] In particular, bulk diamond phase (labeled Si-2) exhibits even-member rings (Si_6) while clathrate lattices exhibit a large number of odd-member rings (87% of Si_5). Despite considerable efforts to characterize the vibrational modes in such clathrate lattices, the models developed to date are not able to reproduce the phonon signature obtained, for example, by Raman spectroscopy.[8–11] Such studies are fundamental to the understanding of the electron-phonon and/or phonon-phonon coupling mechanisms in the superconducting phases. In this paper, we report the first observation of the complete phonon density of states (p-DOS) deduced from inelastic neutron scattering. Two phases (Si-46 and Si-34) have been studied with various concentrations of impurity atoms (Na, K). The main result revealed by this study is a slight energy shift towards lower frequencies of the optical branches and a shift towards higher frequencies of the acoustic branches, with respect to the diamond phase. Both effects lead to a narrowing of the p-DOS width in the clathrates as observed for the e-DOS.[6] In addition, the metal-silicon coupling in doped clathrates versus the impurity concentration and/or the nature of the impurity is clearly shown in the experimental p-DOS.

II. EXPERIMENTAL PROCEDURE

Figure 1 reports both crystal structures (Si-34 and Si-46) in comparison with the silicon diamond phase. The cagelike clusters are easily seen in the view labeled e in Fig. 1. The main crystallographic data are also reported on the Table I. Endohedrally doped clathrates Na_x@Si-34 (Ref. 12) ($x<12$) have been synthesized by thermal decomposition of NaSi under vacuum at temperatures between 610 and 710 K. Upper values of x ($12<x<20$) are obtained by reacting Na_x@Si-34 with sodium vapor in the temperature range 640–670 K. Another phase M_8@Si-46 (M=Na, K) has been synthesized by thermal decomposition of NaSi (or KSi) under argon atmosphere.[13] Prior to the neutron experiments, the samples are carefully characterized using several techniques. The crystallinity of the samples has been studied by x-ray powder diffraction and high-resolution transmission

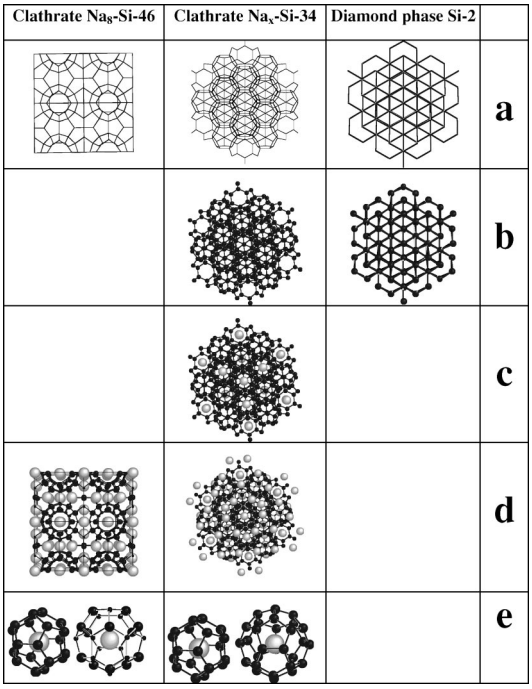

FIG. 1. Selected views of both clathrate lattices in comparison with the silicon diamond phase (labeled Si-2). These lattices are observed perpendicularly to the (111) plane (for Si-2 and Si-34), and to the (100) plane (for Si-46), respectively. (a) shows the lattice frameworks, (b) shows the silicon lattices without alkaline atoms, (c) shows the Na_8@Si-34 lattice with sodium atoms inside the Si_{28} cages, (d) the Na_8@Si-46 (left panel) and Na_{24}@Si-34 (right panel). (e) shows the isolated cages which are the elementary bricks of the clathrate lattices: Si_{20}, Si_{24} (left panel for Si-46 lattice) and Si_{20}, Si_{28} (right panel for Si-34 lattice). The alkaline atoms (Na or K) are showed in light color whereas silicon atoms appear in dark color.

electron microscopy. The chemical purity has been investigated by x-ray microprobe, flame emission, and x-ray photoemission (XPS) spectroscopies. The relative amount of sodium (potassium) has been deduced from the Rietveld analysis of the x-ray diffraction data. These measurements have been corroborated by XPS measurements performed on Na_{1s} (K_{1s}) and Si_{2p} core level lines yielding their ratio. The sodium atoms in the labeled Na_8@Si-34 occupy preferentially the Si_{28} cages whereas the sodium atoms occupy both Si_{20} and Si_{28} cages in the labeled Na_{24}@Si-34 lattice. In the case of Na_8@Si-46 lattice, the sodium atoms occupy both Si_{20} and Si_{24} cages. The inelastic neutron scattering experiments were performed using the high-flux neutron reactor facilities of the Institut Laue-Langevin in Grenoble. The IN6 cold-neutron time-focusing spectrometer was used with an incident wavelength of 4.12 Å (4.8 meV). The maximum of the momentum transfer is 2.6 $Å^{-1}$. The intense beam (8.9×10^4 $cm^{-2}\,s^{-1}$) is extracted by a triple monochromator crystal assembly and time focused by a Fermi chopper. The time-of-flight path is 248 cm length with an angular range from 10° up to 114°. The detection is performed with 337 elliptical ^{3}He detectors. The final spectra were obtained after some corrections including background signal and removal of the signal of the aluminum cell. After summing over the full angular range, one obtains in the incoherent approximation a neutron DOS.[15] Additional backscattered Raman spectra performed on the samples after neutron experiments were measured using a Dilor XY spectrometer and a laser excitation at 647 nm. Details of the Raman study are reported elsewhere.[10]

The clathrate sample formed by a collection of small grains (about 300 mesh) was pressed between two aluminum foils. For comparison, we have studied a silicon diamond powder having the same granularity. All the samples have been studied in the temperature range 100–500 K.

III. RESULTS

A. Si-34 phase

Figure 2 shows the comparison between the p-DOS measured for silicon in the diamond phase (curve *a*) and Na_x@Si-34 clathrate phase ($x=0.6$, see Na_1@Si-34 in Ref. 12) (curve *b*). The spectra reported in Fig. 2 have been obtained at 300 K; however, we have checked that they remain unchanged, except for a trivial temperature factor, in the temperature range from 100 up to 500 K. In the particular case of the clathrate sample used for these measurements (Na_1@Si-34),[12] the purity is high enough (0.7% of Na) to consider the corresponding spectrum (curve *b* in Fig. 2) as representative of a pure silicon clathrate. The signature of the impurity atoms will be discussed below in the case of higher sodium concentration. Finally, it is clear that the neutron energy loss spectrum of the reference sample (Si diamond, curve *a*) is quite similar to the theoretically deduced p-DOS (Refs. 16 and 17) for this phase (Fig. 2). Consequently, we can reasonably rule out a significant influence of the multiphonon processes in our spectra. The low intensity of the transverse opticallike band (labeled OM in Fig. 2) compared to the theoretical p-DOS (Fig. 2) with respect to those of the transverse acousticlike one (labeled AM in Fig. 2) could be assigned to the finite value of the momentum transfer.

Both spectra reported in Fig. 2 for Si diamond and Si clathrate (curves *a* and *b*, respectively) present similar features with three regions attributed to AM, $(A+O)M$, and OM modes.[14] Nevertheless, one observes a slight shift of the optical branches towards lower energy in the clathrate (484 cm^{-1}, 60.0 meV) with respect to the Si diamond one (508 cm^{-1}, 63.0 meV). A similar ''redshift'' is commonly predicted in silicon glass or in liquid state. However, the coordination numbers in these disordered structures are quite different from those in the clathrates and they could not be invoked to explain the ''redshift'' observed. One has to remark that Si-H bands generally located at 117 cm^{-1} (14.5 meV) and 627 cm^{-1} (77.8 meV) (Ref. 18) are not observed in our samples. This is an indication of the very low-hydrogen content adsorbed in the samples. On the other hand, we observe a shift towards higher energies of the AM-like band in clathrate (187 cm^{-1}, 23.2 meV) with respect to the Si diamond one (154 cm^{-1}, 19.1 meV). Moreover, it seems that the acoustic band in Si-34 clathrate is narrower than the one of Si-diamond. Among various plausible explanations, we could mention the isotropy of the cages making up the clathrate lattice.[19] Finally, both above mentioned ''redshifts and blueshifts'' combined lead to a significant reduction of the total p-DOS width in the clathrate compared to the Si diamond. Such a narrowing effect is also observed in the e-DOS and might be attributed to the

TABLE I. Main crystallographic data and selected properties of clathrate: Na_8@Si-46,Na_x@Si-34 and Si-2 diamond lattices, respectively.

Name Notation	Diamond Si-2	Clathrate I Na_x@Si-34	Clathrate II Na_8@Si-46
Space group	$Fd\bar{3}m$	$Fd\bar{3}m$ origin at center $\bar{3}m$	$Pm\bar{3}m$ origin at 4 $\bar{3}m$
Lattice constant	5.4286	14.62	10.235
Position	x,y,z $x,y,z=1/8$	x,y,z (Si) $x,x,x=1/8$ (Si) $x,x,x=0.781$ (Si) $x,y=0.817$; $z=0.629$ (Na) $x,x,x=0$ (Na) $x,x,x=3/8$	x,y,z (Si) $x=1/4$; $y=0$; $z=1/2$ (Si) $x,y,z=0.183$ (Si) $x=0$, $y=0.310$; $z=0.116$ (Na) $x,y,z=0$ (Na) $x=1/4$; $y=1/2$; $z=0$
Number of positions, Wyckoff notation, point symmetry	(Si) 8,a,$\bar{4}3m$	(Si) 8,a,$\bar{4}3m$ (Si) 32,e,3m (Si) 96,g,m (Na) 16,c,$\bar{3}m$ (Na) 8,b,$\bar{4}3m$	(Si) 6,2,42m (Si) 16,i,3 (Si) 24,k,m (Na) 2,a,$m3$ (Na) 6,d,$\bar{4}2m$
Zeolite structure type	none	zeolite ZSM-39	melanophlogite
Type of cages, number per elementary cell	none	$16X\,Si_{20}$ $8X\,Si_{28}$	$2X\,Si_{20}$ $6X\,Si_{24}$
Schoenflies notation	none	$Si_{20}[5^{12}]$	$Si_{20}[5^{12}]$
Schoenflies notation	none	$Si_{28}[5^{12}6^4]$	$Si_{24}[5^{12}6^2]$
Atomic volume at $P=0$ Pa	19.997 Å^3	23.31 Å^3	23.36 Å^3
Hybridization	sp^3	sp^3	sp^3
Mean $d_{Si\text{-}Si}$	2.35 Å	2.38 Å	2.38 Å
Mean deviation in %	0	0.91	0.1
Mean $\theta_{Si\text{-}Si\text{-}Si}$	109,47°	109,4°	109,9°
Mean deviation in %	0	2.8	2.5

poor bonding/antibonding states separation in odd member rings.[6] In fact, from the differences between silicon clathrate and diamond phases, we could expect two contributions to attempt an explanation of the narrowing effect observed in clathrate. First, the perfect sp^3 basis ($d_{Si\text{-}Si}=2.35$ Å, $\theta_{Si\text{-}Si\text{-}Si}=109.47°$ in Si-2) is slightly distorted in the clathrate with a weak spread of first bond lengths and dihedral angles (see Table I) ($d_{Si\text{-}Si}=2.38$ Å, $\Delta d_{Si\text{-}Si}=0.02$Å, $\theta_{Si\text{-}Si\text{-}Si}=109.4°$, $\Delta\theta_{Si\text{-}Si\text{-}Si}=3°$ in Si-34). However, these distortions are weak compared to the ones in amorphous silicon,[17] which still presents broad bands located near 21 meV (170 cm^{-1}) and 60 meV (484 cm^{-1}). A second effect is the topological disorder due to the presence of odd-member rings in clathrate. Previously reported *ab initio* calculations and x-ray photoemission spectra recorded near the Fermi level revealed a wide gap opening of the *e*-DOS in the clathrate compared to the Si-diamond phase.[6] The maxima of the *s*- and *p*-like bands are located near 8 and 1.5 eV in Na_1@Si-34 (9.5 and 2.5 eV in Si diamond), respectively. Since the separation between pure bonding and antibonding states cannot occur in odd member rings, the sp^3 basis is not complete in clathrate despite a nearly perfect tetrahedral symmetry around each Si site. The same problem is encountered in phonon modes. Optical modes are strongly affected by the ring parity while acoustic modes are rather less sensitive. Alben *et al.*[20] have pointed out that the difference between TA and TO modes is correlated to the difference between *p*-antibonding and *p*-bonding functions. Since the separation between both functions is strongly affected in odd-member rings we expect a strong effect in the Si-34 *p*-DOS compared to the Si-2 one. A quantitative understanding of both *OM* and *AM* energy shifts would require first-principles calculations of the phonon spectra while most of the empirical models limited to the first neighbors and ''one particle'' scheme are not suitable. One has to mention that our measured Na_1@Si-34 *p*-DOS presents some striking similarities with the one calculated by Demkov *et al.*[21] From a semi *ab initio* scheme, these authors have found in Si-34 a downward shift of the optical band of 28 cm^{-1} (3,5 meV) with respect to the Si diamond one. Recently, Pederson *et al.*[22] have reported the *p*-DOS calculated for two particular cagelike clusters: Si_{20} and Si_{21}, for which the initial geometry are close to pure and endohedral fullerenes, respectively. The main bands are found around 460 cm^{-1} (57 meV), and 150 cm^{-1} (18.6 meV), in good agreement with our experimental results. *Ab initio* calculations seem to indicate that the *p*-DOS in the silicon clathrate phase is strongly sensitive to the signature of the individual cages.

As for the Raman spectra of both Si-2 and Si-34 crystals presented in Fig. 2, they are quite different because of selection rules which exist in Raman experiments while the absence of such rules in inelastic neutron scattering allows the complete view of the *p*-DOS.

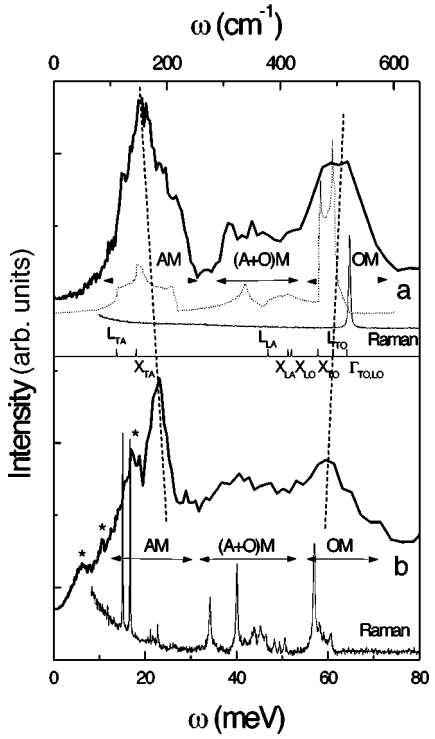

FIG. 2. Phonon density of states deduced from neutron scattering and Raman scattering spectra of (a) silicon diamond and (b) Na_1@Si-34 clathrate phase. (*) on curve (b) mark the peaks corresponding to the sodium p-DOS residual contribution. Calculated phonon frequencies of selected acoustic (AM) and optical (OM) modes as well as frequencies calculated at the high-symmetry points Γ, X, and L by Giannozzi *et al.* (Ref. 16) in the Si-diamond phase are indicated. In addition, the Si-2 diamond p-DOS calculated by these authors is also reported in dashed line (a).

B. Si-46 phase

In addition to the quasi pure Si-34 clathrate phase, we have studied the M_8@Si-46 phase with two different alkali metals: M=Na, K. Both samples have a metalliclike character. Since the potassium atom is larger than the sodium one (atomic radius 2.27 Å , and 1.54 Å for K and Na, respectively), its 4s orbital extends beyond the silicon cage and the overlapping is assumed to be more favorable than for Na_{3s}. The neutron energy loss spectra obtained with both samples Na_8@Si-46 (curve *a*) and K_8@Si-46 (curve *b*) are presented in Fig. 3. The whole spectra is quite different with a significant ''redshift'' of the optical band in K_8@Si-46 with respect to Na_8@Si-46. A similar effect has been observed in Raman spectroscopy by Fang *et al.*[8] Among the plausible explanations, we can mention the Si-Si bond softening effect related with the alkaline-silicon interaction. For such endohedrally doped semiconductor the impurity content as well as the interactions lead to a rise in the position of the Fermi level into the conduction band as predicted by Demkov *et al.*[23] This interaction can be observed directly on the impurity atom signature. The sharp peaks labeled (Na-Si) and (K-Si) in Fig. 3 correspond to the signature of the impurity atoms. Such narrow peaks are close to Einstein-like modes[24] suggesting a narrow electronic density of states as mentioned elsewhere.[23] The energy value of these modes is not affected by the relative concentration of the alkaline. The strong intensity of the sodium peak is related to a large neutron scattering cross section (σ_{Na}=3.28 barn) compared to the potassium one (σ_K=1.98 barn). In addition, the ''alkaline'' vibrational mode is surprisingly located at higher energy for potassium (100 cm^{-1}, 12.4 meV) than for sodium (83 cm^{-1}, 10.3 meV) despite the significantly higher mass of potassium. However, the mass increase is counterbalanced by a better K-Si bonding in K_x@Si_{24} cage since the 4s-(3s3p) overlapping of orbitals is much more efficient than for sodium [3s-(3s3p), respectively]. Unfortunately, we are not able to produce pure Si-46 phase and consequently, the p-DOS reported are dominated by the alkaline-silicon interaction responsible for a softening of the optical modes in M_x@Si-46 with respect to the pure Si-34 phase.

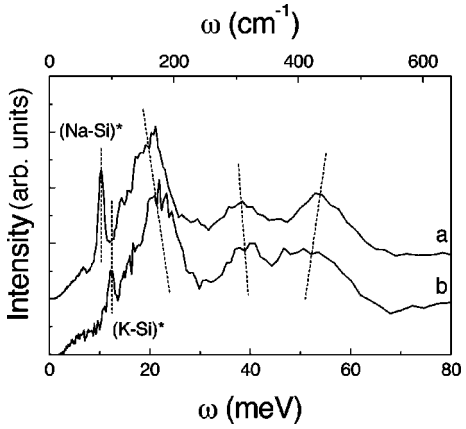

FIG. 3. Phonon density of states deduced from neutron scattering measurements of (a) Na_8@Si-46 and (b) K_8@Si-46. (Na-Si)* and (K-Si)* are the alkaline vibrational modes in Si-46 phase, located at 10.3 meV (83 cm^{-1}) and 12.4 meV (100 cm^{-1}), respectively.

C. Influence of the alkaline

In order to clarify the role of impurities, we studied three doped clathrates (Na_x@Si-34)[12] with $x<1$, $x=8$, and $x=20$, the corresponding neutron scattering spectra of which are reported in Fig. 4. These values correspond to an evolution from an insulating character ($x<1$) towards a metallic behavior ($x=20$), the insulator-metal transition taking place for $x=8$. The sample with $x=20$ contains a significant proportion (27%) (Ref. 12) of the other phase Na_8@Si-46 and has to be discussed carefully. One observes the appearance of a shoulder (labeled # in the Fig. 4) in the acoustic band as the sodium concentration increases. This broadening might be related to two effects. First, the presence of Einstein-like modes at higher energy. This is consistent with sodium located inside the Si_{20} cage. Since the size of the Si_{20} cage is lower than other cages (Si_{24} and Si_{28}), the coupling factor will be more intense leading to high-frequency modes. Second, the shoulder might be also related to an ''*isotropy effect.*''[18] In addition, we observe an increase of the sodium peak intensity with the concentration without significant shift. The presence of two sodium peaks in the spectrum of Na_{20}@Si-34 is attributed to the mixing of both Si-34 and Si-46 phases with non negligible proportions in this sample. The sodium peak appears at a lower energy in Na_1@Si-34 than in Na_8@Si-46 indicating a coupling factor between Na

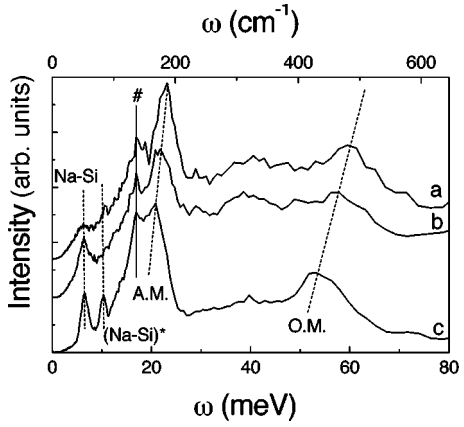

FIG. 4. Phonon density of states deduced from neutron scattering measurements of (a) 95%$Na_{0.6}$@Si-34+5%Na_8@Si-46, (b) 98%Na_8@Si-34+2%Na_8@Si-46, (c) 73%Na_{20}@Si-34 +27%Na_8@Si-46. Sodium vibrational modes: (Na-Si) in Si-34 and (Na-Si)* in Si-46 phase are located at 6.6 meV (53 cm^{-1}) and 10.25 meV (82.7 cm^{-1}), respectively. The band labeled # is also related to the sodium contribution.

and Si smaller in the Si-34 phase than in the Si-46 one. This effect could be related to an increase of the cage size since the sodium occupy Si_{28} cages in Na_x@Si-34 while they occupy Si_{20} and Si_{24} cages in Na_x@Si-46. The behavior of the Na_x@Si-34 p-DOS slightly changes versus the sodium concentration. It seems that we observe a softening of the phonon modes as the sodium concentration increases. This result is consistent with above mentioned results. For $x=20$, the p-DOS changes significantly since we have in this case the superposition of both Na_x@Si-34 and Na_8@Si-46 p-DOS. Nevertheless, we observe similar features between Na_{20}@Si-34 [Fig. 4(c)] and Na_8@Si-46 [Fig. 4(a)]. Consequently, we believe that both clathrate phases (Si-34 and Si-46) present very similar p-DOS.

IV. CONCLUSION

We have reported observation of the full vibrational DOS in two silicon clathrate phases. The interaction between the impurity atom and the silicon skeleton is clearly evidenced in the measured p-DOS. The softening of the Si-Si oscillator strength in K_x@Si-46 compared to Na_x@Si-46 is in good agreement with theoretical predictions. Because of the presence of odd-member rings the phonon-phonon interaction leads to anharmonic effects even at room temperature. Thus, the prediction of the p-DOS requires a complete calculation within a direct first-principle method. Since the clathrate phase requires a large number of atoms per unit cell, this is a good challenge for new semiempirical approach including accurate particle-particle interaction effects.

[1] H. W. Kroto, J. R. Heath, S. C. O'Brien, R. F. Curl, and R. E. Smalley, Nature (London) **318**, 162 (1985).
[2] R. Moret, Phys. Rev. B **48**, 17 619 (1993), and references therein.
[3] J. S. Kasper, P. Hagenmuller, M. Pouchard, and C. Cros, Science **150**, 1713 (1965).
[4] H. Kawaji, H. Hotie, S. Yamanaka, and M. Ishikawa, Phys. Rev. Lett. **74**, 1427 (1995).
[5] G. B. Adams, M. O'Keeffe, A. A. Demkov, O. F. Sankey, and Y.-M. Huang, Phys. Rev. B **49**, 8048 (1994).
[6] P. Mélinon, P. Kéghélian, X. Blase, J. Le Brusq, A. Perez, E. Reny, C. Cros, and M Pouchard, Phys. Rev. B **58**, 12 590 (1998).
[7] S. Saito and A. Oshiyama, Phys. Rev. B **51**, 2628 (1995).
[8] S. L. Fang, L. Grigorian, P. C. Eklund, G. Dresselhaus, M. S. Dresselhaus, H. Kawaji, and S. Yamanaka, Phys. Rev. B **57**, 7686 (1998).
[9] M. Menon, E. Richter, and K. R. Subbaswamy, Phys. Rev. B **56**, 12 290 (1997).
[10] Y. Guyot, B. Champagnon, E. Reny, C. Cros, M. Pouchard, P. Mélinon, A. Perez, and I. Gregora, Phys. Rev. B **57**, R9475 (1998).
[11] D. Kan and J. Lu, Phys. Rev. B **56**, 13 898 (1997).
[12] All the samples are a mixture of both Si-34 and Si-46 phases. For clarity, in the text, we have given to each sample the label of the main phase present in its composition. The complete analysis give the following compositions:
Na_1@Si-34 ($0.95Na_{0.6}$@Si-34+$0.05Na_8$@Si46);
Na_8@Si-34 ($0.98Na_8$@Si34+$0.02Na_8$@Si46);
Na_{20}@Si-34 ($0.73Na_{20}$@Si34+$0.27Na_8$@Si46).
Moreover, in the case of Si-34 lattice, the number of silicon atoms per elementary cell is 136. Thus, the sodium/silicon ratio is 1/136, 8/136, and 20/136 for Na_1@Si-34, Na_8@Si-34, and Na_{20}@Si-34, respectively. In the case of Si-46 lattice, the number of silicon atoms per unit cell being 46, the sodium/silicon ratio is 8/46 in the case of Na_8@Si-46.
[13] E. Reny, M. Ménétrien, C. Cros, M. Pouchard, and J. Sénégas, C. R. Acad. Sci., Ser. II: Mec. Phys., Chim., Sci. Terre Univers **1**, 129 (1998).
[14] We used the terms ''optical'' and ''acoustic'' modes for convenience. In fact, optical and acoustic modes are strictly defined for specific wave vectors. Moreover, owing to the frustration in the clathrate lattice, the optic modes cannot be established. Nevertheless, the labeled ''optic'' and ''acoustic'' bands allow a simple comparison between the clathrate and the diamond lattices.
[15] A. Fontana, F. Rocca, M. P. Fontana, B. Rosi, and A. J. Dianoux, Phys. Rev. B **41**, 3778 (1990).
[16] P. Giannozzi, S. de Giroucoli, P. Pavone, and S. Baroni, Phys. Rev. B **43**, 7231 (1991).
[17] W. A. Kamitakahara, C. M. Soukoulis, H. R. Shanks, V. Buchenau, and G. S. Grest, Phys. Rev. B **36**, 6539 (1987).
[18] L. Cervinka, A. C. Wright, T. M. Brunier, A. C. Hannon, S. M. Bennington, and F. Jansen, J. Non-Cryst. Solids **192-193**, 243 (1995).
[19] M. Widom [Phys. Rev. B **34**, 756 (1986)] has mentioned that the rigidity of the crystal is enhanced for quasicrystal (i.e., icosahedral symmetry) as compared to the fcc lattice (i.e., diamond). Let us remember that the clathrate lattice has a relationship with an icosahedral structure containing a periodic array of disclination lines [J. F. Sadoc and R. Mosseri, J. Non-Cryst. Solids **61-62**, 487 (1984)]. Thus, Widom has shown that soft modes at

low-energy vanish in icosahedron lattice. Consequently, one might observe a shift towards high energy and a narrowing effect in the clathrate acoustic modes. If the introduction of alkali atoms within the cages suppresses the isotropy effect, such soft modes could appear.

[20] R. Alben, D. Weaire, J. E. Smith, Jr., and M. H. Brodsky, Phys. Rev. B **11**, 2271 (1975).

[21] A. A. Demkov, O. F. Saukey, S. Daftvar, and J. Griko, *Proceedings of the 22nd International Conference on The Physics of Semiconductors*, edited by D. J. Lockwood (World Scientific, Singapore, 1994), Vol. 3, p. 2205.

[22] M. R. Pederson, Phys. Rev. B **54**, 2863 (1996).

[23] A. A. Demkov, O. F. Saukey, K. E. Schmidt, G. B. Adams, and M. O'Keeffe, Phys. Rev. B **50**, 17 001 (1994).

[24] R. Brusetti, A. J. Dianoux, P. Gougeon, M. Potel, E. Bonjour, and R. Calemczuk, Phys. Rev. B **41**, 6315 (1990).